Natural convection heat transfer from isothermal horizontal rectangular ducts

O. Zeitoun and Mohamed Ali
King Saud University, Mechanical Engineering Department, P. O. Box 800, Riyadh 11421, Saudi Arabia
Email: ozeitoun@ksu.edu.sa, mali@ksu.edu.sa

Laminar natural convection heat transfer from horizontal rectangular cross section cylinder in air is investigated numerically. Different aspect ratios are examined under laminar conditions. The computational procedure is based on the finite element technique. Results are presented in the form of streamlines, temperature, velocity and heat flux plots around the circumference of the ducts. Heat transfer data are generated and presented in terms of mean Nusselt number versus Rayleigh number for different aspect ratios. Correlation covering the used aspect ratios is obtained in dimensionless form of Nusselt number, Rayleigh number and aspect ratio.

تم دراسة انتقال الحرارة بالحمل الحرارى الطبقى الطبيعى من اسطوانة مستطيلة المقطع لمقاطع ذات نسب جانبية مختلفة عدديا باستخدام طريقة العناصر المحددة. و قد عرضت النتائج على شكل كونتورات لدالة السريان ودرجات الحرارة و توزيعات لدرجات الحرارة و السرعات و الفيض الحرارى. تم الحصول على نتائج لانتقال الحرارة فى شكل رقم نسلت مع رقم رايلى لنسب جانبية مختلفة وقد قورنت هذه النتائج مع العلاقات القليلة المتوفرة لهذا النوع من السريان. تم الحصول على معادلة عامة تمثل العلاقة بين رقم نسلت المتوسط حول الاسطوانة مع رقم رايلى و النسبة الجانبية .

Keywords: Natural convection, Heat transfer, Laminar, Horizontal, Rectangular duct

1. Introduction

Steady state natural convection from rectangular and square ducts has many engineering applications in cooling of electronic components, design of solar collectors and heat exchangers. Survey of the literature shows that correlations for natural convection from vertical and horizontal plates, vertical and horizontal cylinders, spheres, vertical channels and elliptic cylinders are reported for different thermal boundary conditions. However, limited numbers of analytical studies were concerned with heat transfer from the external surface of rectangular and square ducts.

The approximation method suggested by Raithby and Hollands [1] to predict heat transfer from cylinders of various cross sections and for wide ranges of Prandtl and Rayleigh numbers was simplified by Hassani [2]. The free convection from a horizontal cylinder with cross section of arbitrary shape was theoretically analyzed for uniform surface temperature and uniform surface heat flux by Nakamura and Asako [3]. They also checked their theoretical results by experiments in water on long cylinders of modified triangular and square cross section. However, their experimental values of the mean heat transfer coefficient were about 10 to 30 percent higher than the analytical values. Hassani [2] introduced an expression for predicting natural convection from isothermal two-dimensional bodies of arbitrary cross section. His results compared with the experimental ones of Nakamura and Asako [3] for the modified square cross section in water with an rms difference of 8.4 percent. Hassani's [2] results were also compared with the experimental data of Osthuizen and Paul [4] for cylinder with square cross section in air.

The objective of the present study is to use the complete Navier-Stokes equations and the energy equation to solve the natural convection problem about a noncircular isothermal ducts (rectangular and square) for different aspect ratios in air numerically. The solutions are obtained for a wide range of Rayliegh number and Nusselt number. Correlation is

obtained for Nusselt number using Rayleigh number and the aspect ratio.

2. Mathematical formulation

The governing two dimensional dimensionless equations in a cartesian coordinate system for steady, incompressible, laminar flow with negligible viscous dissipation and constant property fluids except the density are given by:

$$\Gamma \frac{\partial u}{\partial x}+\frac{\partial v}{\partial y}=0\,, \tag{1}$$

$$\Gamma u\frac{\partial u}{\partial x}+v\frac{\partial u}{\partial y}=-\Gamma\frac{\partial P}{\partial x}+\kappa\left[\Gamma^2\frac{\partial^2 u}{\partial x^2}+\frac{\partial^2 u}{\partial y^2}\right], \tag{2}$$

$$\Gamma u\frac{\partial v}{\partial x}+v\frac{\partial v}{\partial y}=-\frac{\partial P}{\partial y}+\kappa\left[\Gamma^2\frac{\partial^2 v}{\partial x^2}+\frac{\partial^2 v}{\partial y^2}\right]+\frac{\rho_\infty}{\rho}\frac{Gr}{\kappa}\,\theta, \tag{3}$$

$$\Gamma u\frac{\partial \theta}{\partial x}+v\frac{\partial \theta}{\partial y}=\frac{\kappa}{Pr}\left[\Gamma^2\frac{\partial^2 \theta}{\partial x^2}+\frac{\partial^2 \theta}{\partial y^2}\right]. \tag{4}$$

The boundary conditions for the present problem are specified as follows fig. 1:
- on the symmetric vertical y-axis:

$$u = 0,\ \frac{\partial v}{\partial x}=\frac{\partial \theta}{\partial x}=0\,, \tag{5}$$

- on the bottom boundary:

$$u = v = \theta = 0, \tag{6}$$

- on the top boundary:

$$\frac{\partial u}{\partial y}=\frac{\partial v}{\partial y}=\frac{\partial \theta}{\partial y}=0\,, \tag{7}$$

- on the far field x-direction boundary:

$$u = v = \theta = 0, \tag{8}$$

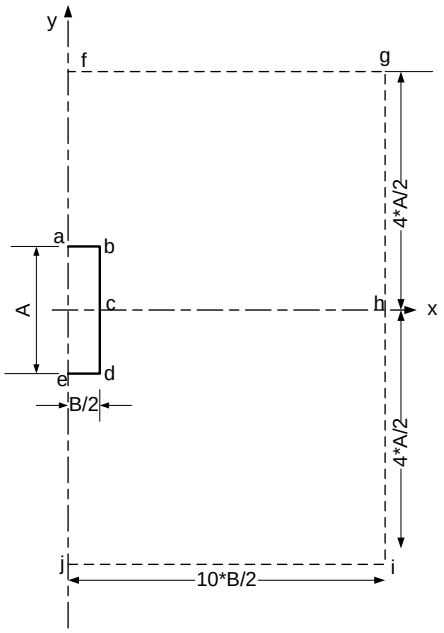

Fig. 1. Dimensions of the solution domain where A and B are the duct's dimensions.

- on the isothermal surface of the body:

$$u = v = 0,\ \theta = 1. \tag{9}$$

It should be mentioned that in this analysis the ideal gas equation of state (not the Boussinesq approximation) provided by the software is used as an input for estimating the density of the fluid. The equations are made dimensionless by choosing the scales [B, A, U, ΔT, ρU^2] for length in x-dir., length in y-dir., velocities, temperature and pressure, respectively. Here $U = \nu / L$ is a characteristic velocity, L is a characteristic length, $\Delta T = T_w - T_\infty$ is the temperature difference and A and B are the height and width of the cross section of the duct. The dimensionless parameters $Gr = g\,\beta\,\Delta T\,L^3 / \nu^2$, $Pr = \nu/a$, $\Gamma = A/B$, $\kappa = L/A$ appearing in the equations are the Grashof, Prandtl numbers, aspect ratio and the length scale ratio, respectively. It should be mentioned that the aspect ratio and the length scale ratio appearing in the equations are due to using different normalization for the length scales in x and y directions.

The solution domain is seen in fig. 1 where the flow is symmetric about the vertical y-axis

therefore, only one half of the rectangular or square section will be considered. It should be noticed that, the far field value in the x-direction is chosen ten times of $B/2$ from the lines of symmetry. Also the far field value in positive or negative y-direction is taken four times of $A/2$ from the horizontal x axis where A and B are the cross section dimensions of the duct. It should be noticed that, the far field x and y direction boundaries are assumed to be far enough from the hot duct surface to be unaffected by heating and natural convection circulation. This assumption is checked by changing the calculated domain around the duct until satisfied conditions are obtained. This procedure is first applied to a horizontal cylinder and it was found that putting far field right, lower and upper boundaries at 5D, 2D and 2D respectively gave good results as shown later and is adopted here for the non circular ducts.

3. Numerical solution procedure

The governing eqs. (1-4) are solved numerically using Cosmos-Flow Plus software which was derived from the SIMPLER solution scheme introduced by Patankar [5]. This software is recently used by Zeitoun [6] to study the heat transfer and flow fields by natural convection from a vertical plate enclosed in a horizontal cylinder. This code uses the finite element method to obtain approximate solutions to the boundary value problems. By using this method, the governing partial differential equations are reduced to a set of algebraic equations. The dependent variables are represented by polynomial shape functions over a small area or volume (element). These representations are substituted into the governing equations and then the weighted integral of these equations over the element is taken where the weight function is chosen to be the same as the shape function. The result is a set of algebraic equations for the dependent variable at discrete points or nodes on every element. By assuming a simple form of solution in each finite element, the approximate solution of the problem in the complete domain is determined. The pressure-velocity coupling problem is solved by using the well known SIMPLER method [5] where the pressure is first solved using the assumed velocity components. Velocity correction equations are then solved to correct the velocities. The pressure and velocity fields are then corrected based on the calculated values of pressure and velocities. This process is repeated until the residual of all equations are negligible. Similar routine is used by Al-Sanea and Ali [7] to obtain the heat transfer and flow fields near the extrusion slit of a continuously moving surface.

A four node quadrilateral element type was used in the current investigation. The numerical results are checked for grid independency by increasing the number of nodes till a stage is reached where the results produce negligible changes with further refinement in grid size. Based on that the solution domain is divided into number of nodes such that: 100 nodes along the lines *af*, *bg*, *ch*, *di*, and *ej* and 45 nodes along the lines *ab*, *bc*, *cd*, *de*, *fg*, *gh*, *hi*, and *ij* as seen in fig. 1. These distributions of nodes, as seen in fig. 2, make the grid points denser near the surface

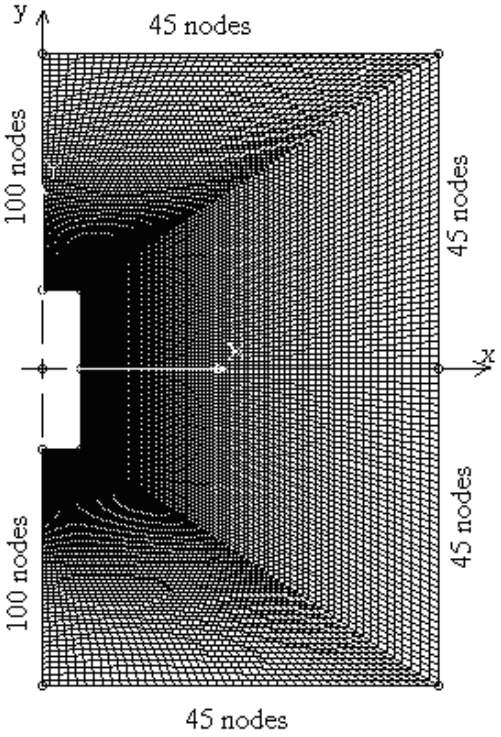

Fig. 2. The meshing system of the solution domain showing the number of nodes.

boundary of the body where the changes in velocity and temperature can be traced out more accuratly. The solution dependency on grid number is checked out as follows: first, the duct surface circumference nodes are fixed at 180 and the number of nodes is varied from 50, 75 to 100 along the lines *af*, *bg*, *ch*, *di*, and *ej* (see fig. 1). Secondly, the number of nodes along the rays specified earlier are fixed at 100 nodes and the nodes at the circumference are varied from 100, 140 to 180 as seen in table 1 for $\Gamma = 1$ and for $\Delta T = 10$ K. In each case the percentage change in the heat flux per unit length is calculated and reported in table 1. Upon these tests, a grid system of 180 (on the circumference) ×100 (rays) is found to give good results and consequently is used in the current analysis.

The current numerical model is validated by solving natural convection around a horizontal cylinder. The flow around the right half of the cylinder is only solved due to symmetry of the problem. The far field boundaries are chosen as discussed before. The solution dependency on grid number has been examined. Furthermore, using 180 grids along half of circumference of the cylinder and 100 grids along the radial direction, with denser nodes at cylinder surface, is found to give accurate results. Heat transfer data from the cylinder surface, presented by Nuuselt number, are compared to the available data in the literature. fig. 3 shows the comparison between the numerical results obtained by Kuehn and Goldstein [8] with the present results for free convection about a horizontal isothermal cylinder in air. The current results for a wide range of Rayleigh number and for two different cylinders are compared with the numerical results of [8] and the comparion shows shows very good agreement as seen in fig. 3. Furthermore, the present results compared well with the numerical results of Chouikh et al. [9]. Comparison between current results about isothermal cylinder and correlations of Churchill and Chu [10] and Morgan [11] are shown in fig. 4. The comparison shows very good agreement as shown in fig. 4.

4. Results and discussions

The current problem is solved for air and the run conditions are summarized in Table 2. Several solutions are obtained for $3.31 \times 10^4 \leq Ra \leq 5.17 \times 10^7$ and for aspect ratios $\Gamma = 0.25$, 0.5, 1, 2 and 4.

Sample of isotherms and streamlines for different aspect ratios are shown in figs. 5 and 6, respectively, for different aspect ratios. It can be seen in these figures that the isotherms hugs the surface boundary at the bottom and vertical sides of the surface where the thermal boundary layer thickness is thinner than that at the top surface of the body. These figures show also the effect of the aspect ratio on the streamlines and isotherms especially near the top surface of the body. For example; at $\Gamma = 4$ the flow separation from the top surface of the body is observed in fig. 6-c. On the other hand there is no flow separation for the aspect ratios of 0.25 as seen in fig. 6-a.

The temperature and velocity profiles along the x-axis, positive y-axis and negative y-axis along the centerline of the duct are shown in fig. 7-a to 7-c for two Rayleigh numbers of 9.53×10^4 and 3.31×10^6 for square duct of $\Gamma = 1$. The effect of increasing Rayleigh number on decreasing the thermal boundary layer is clear in these figures. However, on the top surface the distance which the temperature should take to reach the ambient temperature is slightly affected by Rayleigh number as shown in fig. 7-b. The reason for that could be seen from the isotherms in fig. 5 for example where the ambient isothermal lines is almost parallel to the y-axis and the temperature profile along the positive y-axis is constrained by our top boundary of the solution domain. Therefore, one can notice that the gradient of the temperature is approximately zero at the edge of the thermal boundary layer for figs. 7-a and 7-c where the temperature profiles go asymptotically to zero. On the other hand, the temperature at the end of the solution domain in fig. 7-b is not zero since the plume is still rising with a temperature greater than the ambient temperature.

Table 1
Effect of grid number on the solution results

A= 0.1 m B =0.1 m ΔT=10 K	Effect of grid number variation in af, bg,ch, di, and ej directions (see Fig. 1)			Effect of grid number variation along the circumference direction		
	Meshing	Q, W/m	$\Delta Q/Q$%	Meshing	Q, W/m	$\Delta Q/Q$%
	50x180	15.7932	-1.99263	100x100	16.284	1.08143
	75x180	16.1385	0.189609	100x140	16.1433	0.219286
	100x180	16.1079	0	100x180	16.1079	0

Table 2
Run conditions

Γ	A, m	B, m	T_w, K	T_∞, K
0.25	0.005	0.02	300.1	300
	0.01	0.04		
	0.02	0.08	to	
	0.05	0.2		
0.5	0.01	0.02	400	
	0.05	0.1		
	0.1	0.2		
1	0.01	0.01		
	0.02	0.02		
	0.05	0.05		
	0.1	0.1		
2	0.02	0.01		
	0.1	0.05		
	0.2	0.1		
4	0.02	0.005		
	0.04	0.01		
	0.08	0.02		
	0.2	0.05		

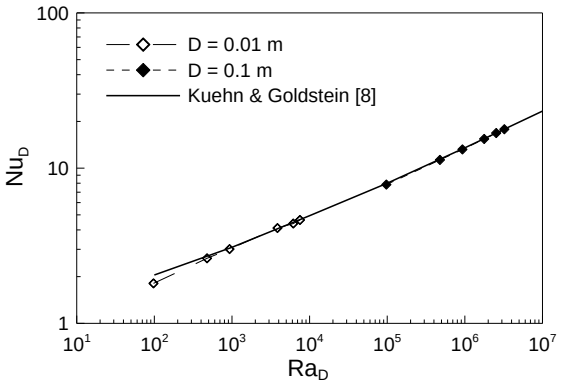

Fig. 3. Comparison with Kuehn and Goldstein [8] for natural convection about isothermal cylinder in air for two different diameters.

Fig. 7-a shows that as Rayleigh number increases the velocity boundary layer thickness decreases and the maximum vertical velocity is shifted towards the surface of the body. The negative velocities appearing in the figure indicate that the flow is going towards the vertical surface of the square as indicated from the streamlines in fig. 6.

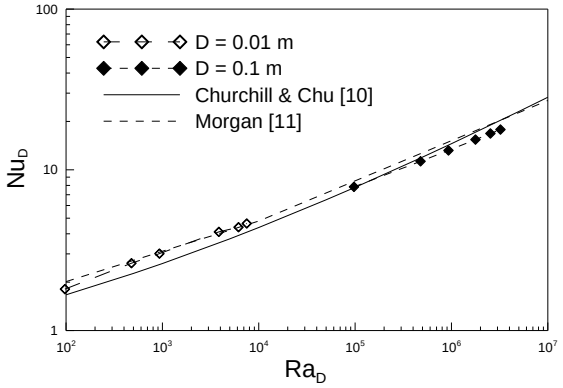

Fig. 4. Comparison with correlations of natural convection about isothermal cylinder.

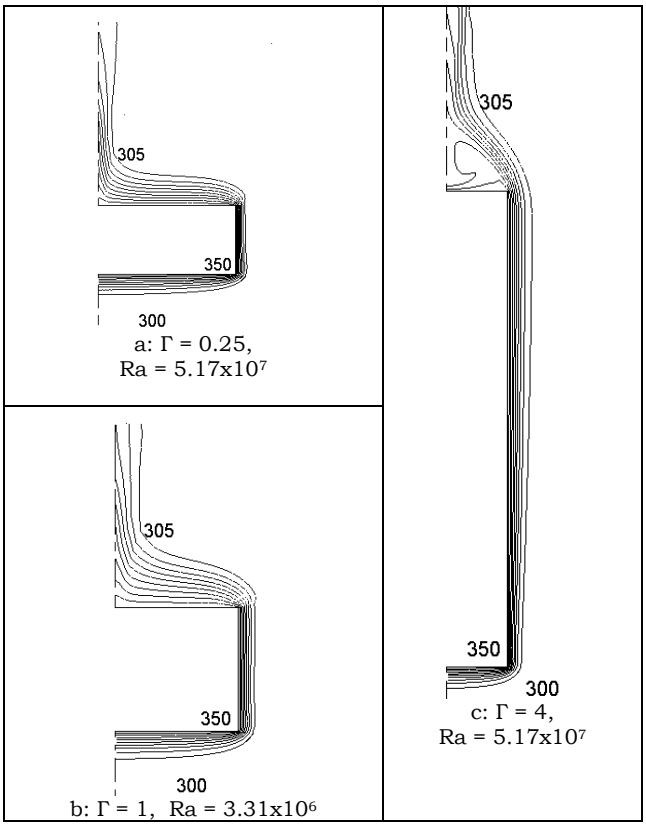

Fig. 5. Temperature contours.

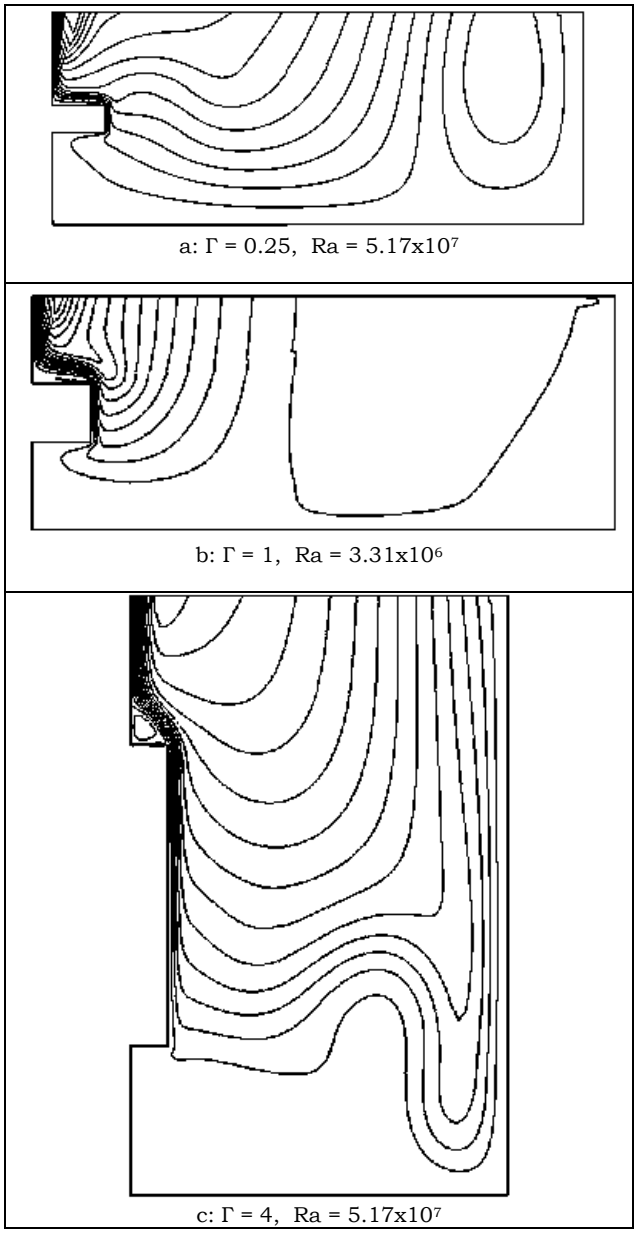

Fig. 6. Stream lines.

Fig. 7-b shows the velocity profiles at the center line in the positive y-axis where the effect of increasing Ra is to increase the separation and the strength of the reverse flow very close to the top surface. However, beyond this, the velocity increases as the y-axis increases since the plume is rising and this center line velocity is the largest velocity in the plume. Fig. 7-c illustrates the velocity profiles at the center line in the negative y-axis. The velocity in this section is fairly small since the fluid is supposed to be stratified and hence stable and the effect of increasing Ra is to increase the maximum velocity and to shift it towards the bottom surface.

The total heat transfer from the duct surface is calculated by integrating the local heat flux along the circumference of the duct,

$$Q = \int_{A_i} q_w dA\,, \tag{10}$$

where the local heat flux is estimated by applying Fourier's law at the surface of the duct,

$$q_w = -k\frac{\partial T}{\partial n}|_w\,, \tag{11}$$

where n is the outward normal to the wall. Samples of heat flux distributions along the sides of duct are shown in figs. 8 and 9. As shown in the figures, the heat flux increases from symmetry axis along the bottom surface where it reaches maximum values at the bottom corner of rectangle cross section. For the upper surface, the heat flux starts with high value at symmetry axis, then decreases and finally increases near the upper corner due to sharp decrease in thermal boundary layer as shown in fig. 5. The heat flux decreases slightly along the vertical side except at corners. The heat flux is higher at the lower corner because the thermal boundary is thinner at the lower corner, see fig. 5.

The average Nusselt number based on the duct characteristic length L is expressed as $Nu=hL/k$. Here, h is the average heat transfer coefficient along the circumference of duct and is calculated from,

$$h = \frac{Q}{(T_w - T_\infty)A_s}\,. \tag{12}$$

The predicted Nusselt number is plotted versus Rayleigh number for various aspect ratios Γ = 0.25, 0.5, 1.0, 2, and 4.0 as shown in Fig. 10. As it is expected, Nusselt number increases as Rayleigh increases. However, the

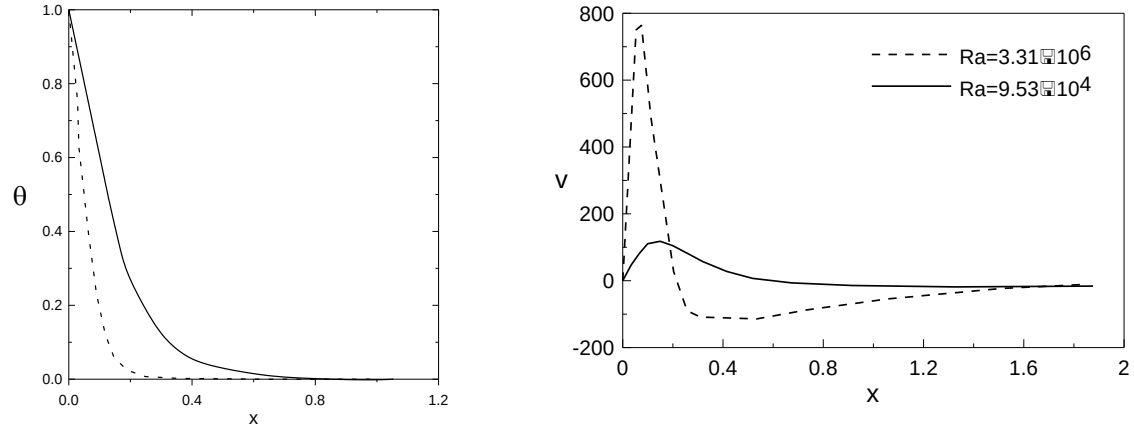

(a) along the x- axis

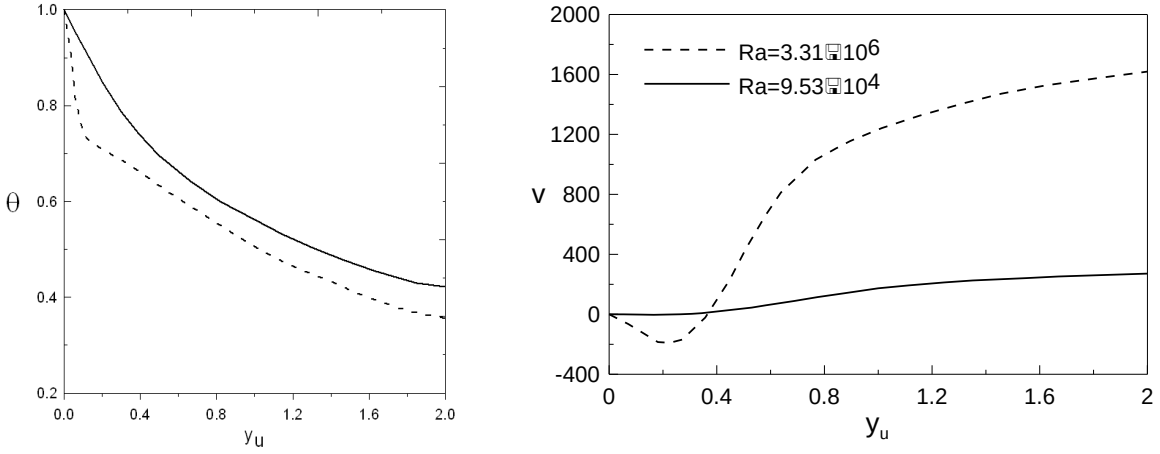

(b) along the vertical upward y- axis

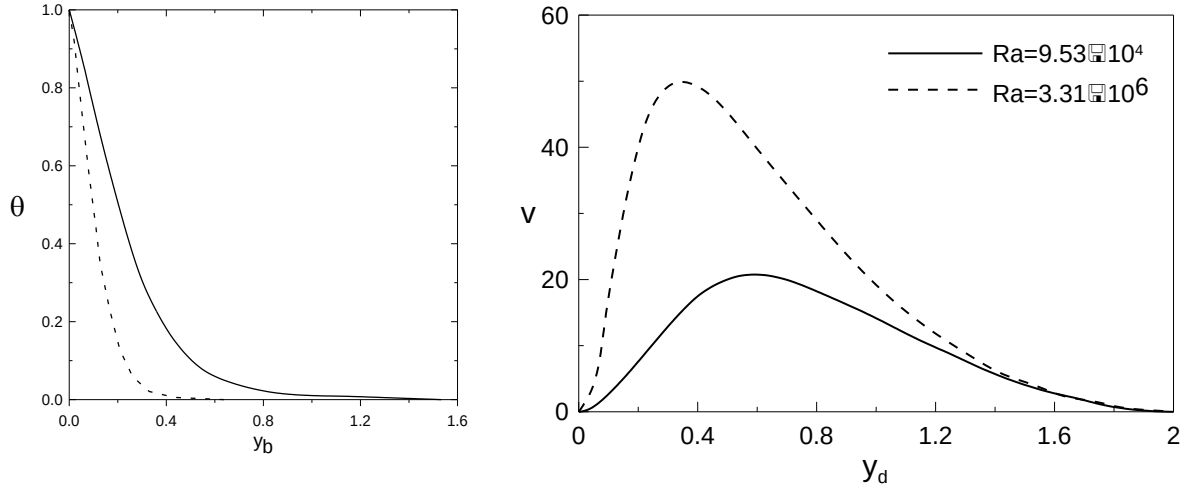

(c) along the vertical downward y- axis

Fig. 7. Temperature and velocity profiles for Ra = 3.31 × 10^6 for square duct cross section of Γ= 1.

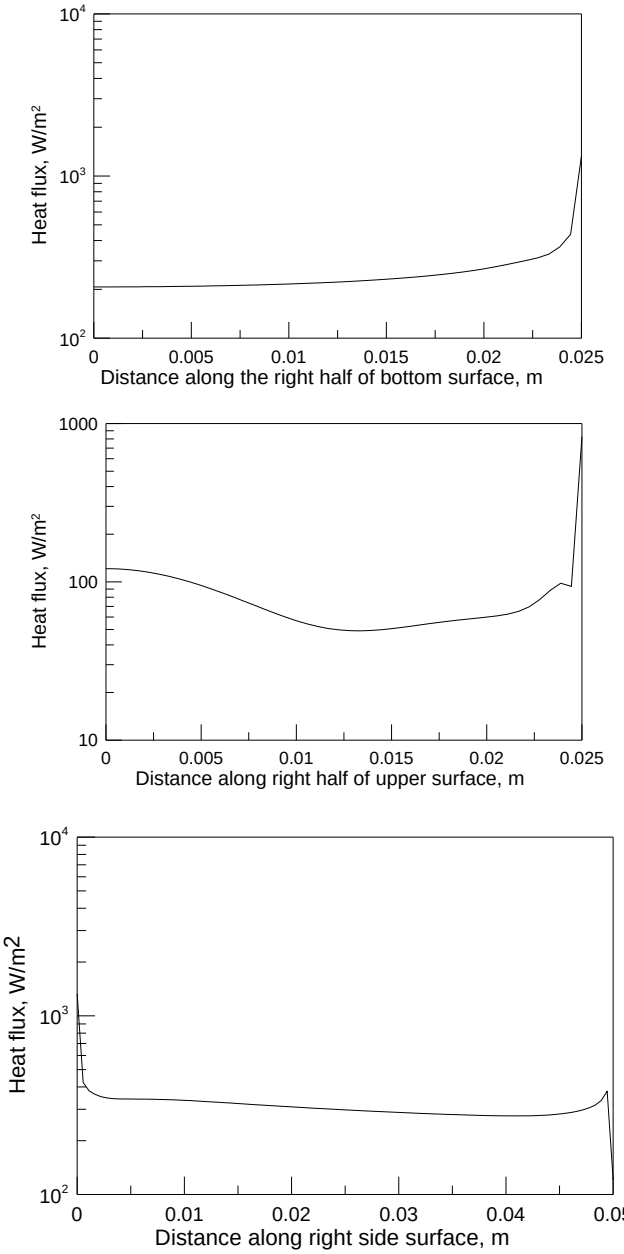

Fig. 8. Heat flux along surface of a duct of A=i=0.05 m for ΔT = 50°C.

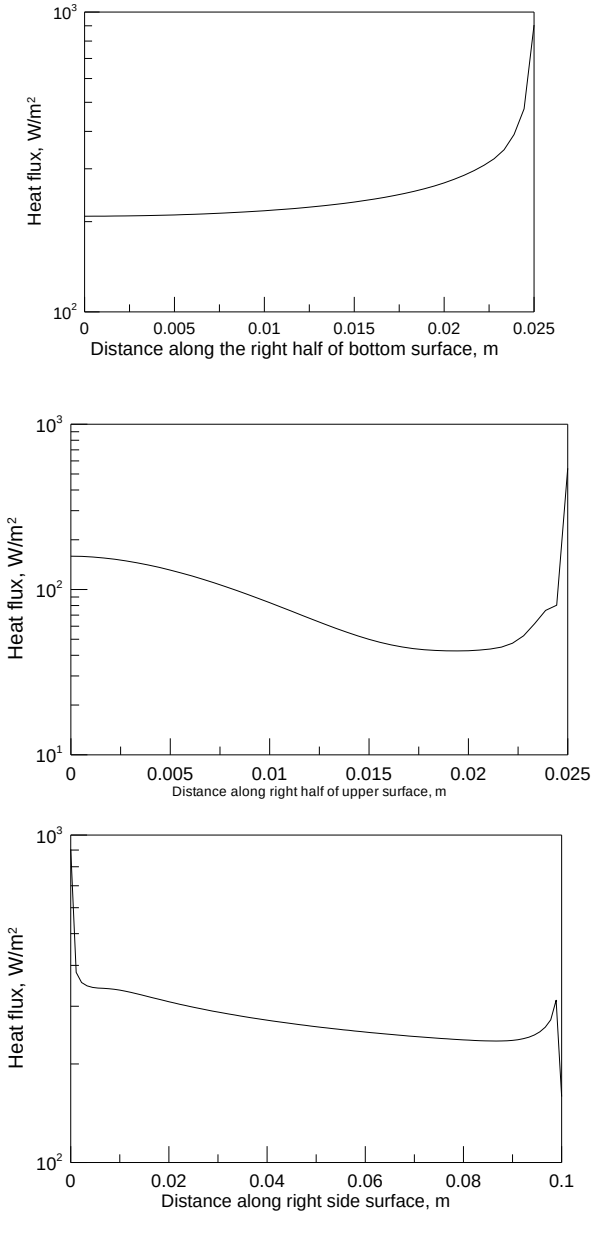

Fig. 9. Heat flux along surface of a duct of A= 0.1 m and B=0.05 m for ΔT = 50°C.

Nusselt number is higher for duct of high aspect ratio.

The present results for square duct in air are compared with the predicted analytical correlation of Hassani [2] for free convection about long cylinder of modified square cross section as seen in fig. 11 for Γ = 1. As seen in the figure, the present numerical results are lower 15% compared to the prediction of the correlation of Hassani [2].

Using $L = A + B$ as a characteristic length, the data presented in fig. 10 are correlated using Nu, Ra and Γ and the best fitting curve through this data is obtained as:

$$Nu = \left[\begin{array}{l} 0.9\ \Gamma^{-0.061} + \\ 0.371\ \Gamma^{0.114} Ra^{0.1445} \end{array} \right]^2 . \qquad (13)$$

$$700 \le Ra \le 10^8$$

The correlation coefficient of above correlation is R=99.8%. The correlated Nusselt number $Nu_{Corr.}$ from eq. (13) is plotted against the exact Nusselt number Nu_{Num} obtained from the numerical results in fig. 10. The solid line in fig. 12 represents the perfect match and the error bands are – 4 % to + 10 %, where most of the data (at least 95 %) fall within this band.

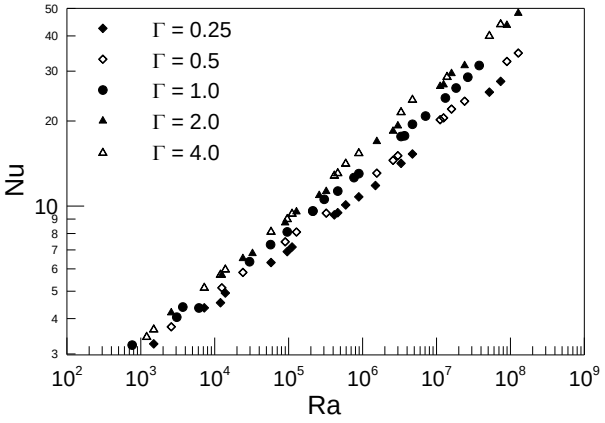

Fig. 10. Numerical values of Nusselt number verses Rayleigh number for different aspect ratios.

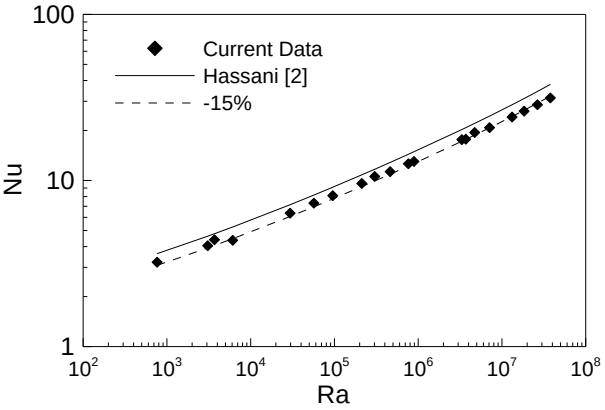

Fig. 11. Comparison with Hassani [2] for free convection about long cylinder of modified square cross section in air.

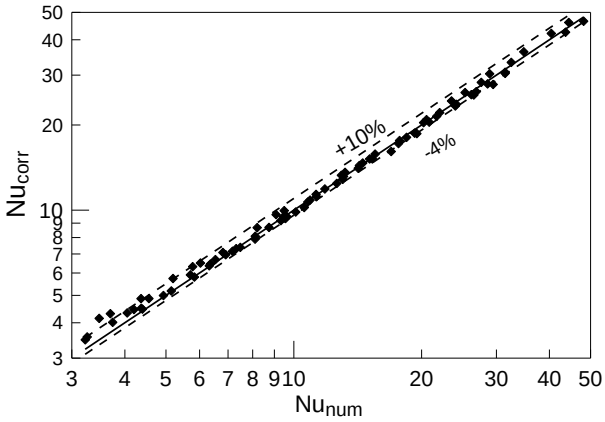

Fig. 12. Comparisons between prediction of proposed correlations and numerical data.

5. Conclusions

Natural convection from square and rectangular cross section ducts has been investigated for wide ranges of Rayleigh number and duct aspect ratio. Streamlines show that for fixed Rayleigh number as the aspect ratio increases; separation and circulation occurs above the top surface of the duct and the corresponding behavior was observed through the isotherms. Furthermore, It was found that increasing Rayleigh number reduces the thermal boundary layer along the vertical and bottom surface of the duct. However, on the top surface, at the center line, where the plume is rising; increasing *Ra* has a weak effect on the thermal boundary layer and its thickness depends on the chosen solution domain. Velocity distributions were also presented and the circulation and reverse flow observed by the streamlines were depicted by the velocity profiles. The total average heat fluxes around the circumference are computed and the average heat transfer coefficients are expressed in dimensionless form as Nusselt number for various aspect ratio. Finally, correlation (eq. (13)) covering wide ranges of Rayleigh number for various aspect ratio is obtained for horizontal square and rectangular cross section ducts.

Nomenclature

A is the duct height, m,
A_s is the surface area, 2(A+B)l, m^2,

B is the duct width, m,
Gr is the Grashof number, $= g\beta\Delta T L^3/\upsilon^2$,
k is the thermal conductivity, W/m K
L is the characteristic length, $= A + B$, m,
l is the duct length, m,
Nu is the Nusselt number,$= hL/k$,
P is the pressure, Pa,
Pr is the Prandtl number, $= \upsilon/a$,
Ra is the Rayleigh number, $= g\beta\Delta T L^3/\upsilon a$,
ΔT is the temperature difference,$= T_w - T_\infty$, K
U is the characteristic velocity,$=\upsilon/L$, m/s,
u is the dimensionless velocity component in x direction,
υ is the dimensionless velocity component in y direction,
x is the dimensionless horizontal coordinate, and
y is the dimensionless vertical coordinate.

Greek symbols

Γ is the aspect ratio $= A/B$,
a is the thermal diffusivity, m^2/s,
β is the thermal expansion coefficient, K^{-1},
θ is the dimensionless temperature, $= \dfrac{(T - T_\infty)}{(T_w - T_\infty)}$
υ is the kinematic viscosity, m^2/s,
κ is the length scale ratio, L/A, $=(1+ \Gamma^{-1})$, and
ρ is the density, kg/m^3.

Subscripts

u is the upward direction,
d is the downward direction,
w is the at the surface, and
∞ is the ambient condition.

References

[1] G.D. Raithby, and K.G.T. Hollands, "A General Method of Obtaining Approximate Solutions to Laminar and Turbulent Free Convection Problems" Advances in Heat Transfer, eds. T.F. Irvine Jr. and J.P. Hartnett, Academic Press, New York, Vol. 11, pp. 265-315 (1975).

[2] A.V. Hassani, "Natural Convection Heat Transfer from Cylinders of Arbitrary Cross Section", ASME, J. Heat Transfer, Vol. 114, pp. 768-773 (1992).

[3] H. Nakamura, Y. and Asako, "Laminar Free Convection From A Horizontal Cylinder With Uniform Cross Section of Arbitrary Shape", Bull. JSME, Vol. 21 (153), pp. 471-478 (1978).

[4] P.H. Osthuizen, and J.T. Paul, "An Experimental Study Of Free Convection Heat Transfer From Horizontal Non-Circular Cylinders", the 22nd National Heat Transfer Conference, Niagara Falls, New York, ASME Heat Transfer Division, Vol. 32, pp. 91-97 (1984).

[5] S.V. Patankar, Numerical Heat Transfer and Fluid Flow, Hemisphere (1980).

[6] O. Zeitoun, "Natural convection from a vertical plate in a horizontal cylinder", Int. J. of heat and Technology, Vol. 23 (1) (2005).

[7] S.A. Al-Sanea, and M.E. Ali, "The effect of Extrusion slit on the Flow and Heat Transfer Characteristics from a Continuously Moving Material with Suction or Injection", Int. J. Heat and Fluid Flow, Vol. 21 (1) pp. 84-91 (2000).

[8] T.H. Kuehn, and R.J. Goldstein, "Numerical Solution to the Navier-Stokes Equations for Laminar Natural Convection About a Horizontal Isothermal Circular Cylinder", Int. J. Heat Mass Transfer, Vol. 23, pp. 971-979 (1980).

[9] R. Chouikh, A. Guizani, and M. Maalej, "Numerical Study of the Laminar Natural Convection Flow Around Horizontal Isothermal Cylinder", Renewable Energy, Vol. 13 (1), pp. 77-88 (1998).

[10] S.W. Churchill, H.H.S. and Chu, "Correlating Equations for Laminar and Turbulent Free Convection from a Horizontal Cylinder", Int. J. Heat Mass Transfer, Vol. 18, pp. 1049-1053 (1975).

[11] V.T. Morgan, "The overall convective heat transfer from smooth circular cylinders", Advances in Heat Transfer, eds. T.F. Irvine Jr. and J. P. Hartnett, Academic Press, New York Vol. 11, pp. 199-264 (1975).

Received July 23, 2005
Accepted August 13, 2005